A SIMPLE INSTRUMENT FOR MEASURING THE LIGHT-INDUCED BIREFRINGENCE IN A PHOTOREFRACTIVE CRYSTAL

Ruey-Ching Twu,[1] Yi-Fan Chu,[2] and Ming-Tsung Hsu[1]
[1] Department of Electro-Optical Engineering, Southern Taiwan University, Tainan 710, Taiwan; Corresponding author: rctwu@mail.stut.edu.tw
[2] Institute of Nanotechnology, Southern Taiwan University, Tainan 710, Taiwan

Received 17 May 2010

ABSTRACT: *We present a simple homodyne phase measurement instrument to evaluate a light-induced birefringence change in an Mg-doped congruent lithium niobate crystal by using an integrated lithium niobate Zn-indiffused phase modulator (ZIPM) for optical signal modulations. The results successfully demonstrate that the focused beam and modulated phase of the ZIPM can provide a simple pump-probe method for measuring the evolutions of light-induced birefringence changes. The detection of birefringence change at the level of* 10^{-7} *is lower than the conventional Senarmont compensation method.* Microwave Opt Technol Lett 53:367–369, 2011; View this article online at wileyonlinelibrary.com. DOI 10.1002/mop.25702

Key words: *photorefractive; lithium niobate; homodyne phase measurement*

1. INTRODUCTION

Photorefractive materials have been extensively studied because of a wide variety of applications in areas including optical holograms, nonlinear-optical applications, and photoinduced optical waveguides [1−5]. Traditionally, the photosensitivity of a photorefractive crystal was measured by using a two-beam coupling method. The dynamical formations of spatial phase gratings due to the photorefractive effect (PRE) can be monitored by measuring the temporal diffraction efficiency of a probe light [2]. Besides, the light-induced space-charge electric field will modulate the refractive indices to make a birefringence change in the photorefractive crystals. The phase retardations between input orthogonal polarizations passing through such crystals can be measured using a common-path polarization interferometer based on the Senarmont compensation method [6, 7]. Usually, these dynamic behaviors can be observed by using a single visible-wavelength laser with enough power intensity. Moreover, a pump-probe technique with two different-wavelength lights was also proposed in the past decade [6, 7].

In this article, a simple instrument is proposed to study the light-induced birefringence change in an Mg-doped congruent $LiNbO_3$ (5 mol% Mg:LN) crystal. The approach is similar to the previous dual-channel phase measurement setup [8]. An integrated lithium-niobate Zn-indiffused phase modulator (ZIPM) as reported in [9] was used to modulate the incident light phase for further spectrum analysis in the homodyne interferometer. The phase information is then extracted by the Fourier analysis of the odd and even harmonics of the output signal. Because a diameter of output beam from the ZIPM passing through an objective lens is 80 μm, it is easy to make a high-intensity light at a wavelength of 633 nm. The narrow-diameter and high-intensity light beam easily builds up a strong space-charge field to cause obvious PRE in the test Mg:LN crystal. Thus, the focused beam with phase modulation can provide the pump and probe purposes for characterizing the birefringence changes. Besides, the birefringence behaviors can be modulated by irradiating the beam with another pump light at a 532-nm wavelength. Because the temporal variations of birefringence changes are slow, the modulation speed 100 Hz of the ZIPM is enough to obtain a sensitivity measurement. Actually, it is easy to operate in high speeds of over MHz with prompt electrode designs for improving measurement response.

2. EXPERIMENTAL SETUP AND MEASUREMENTS

Figure 1 illustrates the proposed novel light-induced birefringence measurement setup. The ZIPM was made by using a Zn-strip of 4-μm wide, and 35-nm thick with predeposition Ni film of 6 nm under the thermal diffusion of 850°C for 150 min. The fabricated waveguide is single mode for both TE and TM polarizations. After thermal diffusion and end faces polished, a silicon dioxide (SiO_2) buffer layer of 300 nm was deposited. Then, an Al electrode of thickness 300 nm was deposited and patterned. The gap width between parallel electrodes is 24 μm, and the electrode length is 15 mm. A He–Ne laser (R-Laser) with a 633-nm wavelength is used, and the power is controlled by adjusting the transmission angles between two polarizers (PL1 and PL2). By controlling the rotation angles of a half-wave plate, the linearly-polarized light at an azimuth angle of +45° was launched into the ZIPM through a 40× objective lens (L1). The output waveguide modes were collimated through another 40× objective lens (L2). The focused beam sizes can be changed by adjusting the distance between the ZIPM and L2. The scattering lights can be filtered out by using a pinhole with an aperture diameter of 0.1 mm. Then, the nonpolarization beam splitter (BS1) is used to spatially separate the modulated light beam from the ZIPM. The reflected light is a reference signal for monitoring the phase stabilities of the ZIPM. The transmitted one is a sensing signal for measuring the light-induced

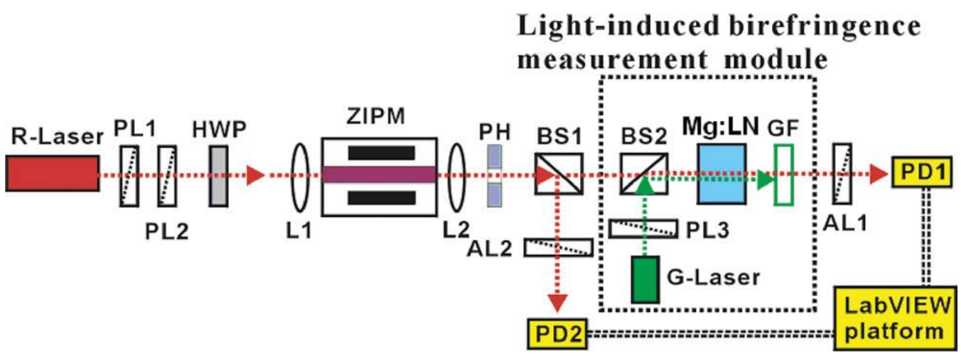

Figure 1 Schematic of experimental setup for a light-induced birefringence measurement. [Color figure can be viewed in the online issue, which is available at wileyonlinelibrary.com]

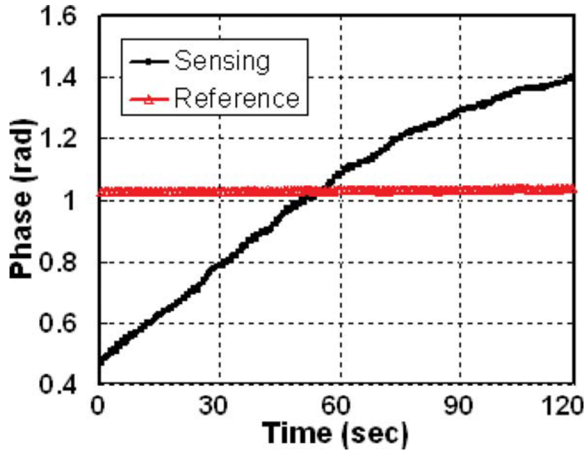

Figure 2 Phase variations as a function of time for the sensing and reference channels. [Color figure can be viewed in the online issue, which is available at wileyonlinelibrary.com]

birefringence change after passing through the Mg:LN crystal. To modulate the PRE, the pump light from a diode-pumped solid-state laser of 532-nm wavelength (G-Laser) is launched to the Mg:LN crystal, after passing through the BS2. The input extraordinary polarization is adjusted with a polarizer PL3. Behind the Mg:LN crystal, the output pump light is blocked by using an optical filter GF. Therefore, both the sensing and reference signals were received by the photodetectors PD1 and PD2 after passing through the analyzers AL1 and AL2 at the same azimuth angles of $+45°$, respectively. The signal process and real-time display were performed in the LabVIEW platform (National Instruments) as proposed in [8]. By considering the z-cut/x-propagation Mg:LN crystal, the light-induced refractive index changes of the extraordinary (Δn_e) and ordinary (Δn_o) polarizations that are represented by

$$\Delta n_{e,o} = -(1/2) n_{e,o} r^3_{33,13} E_{PR} \tag{1}$$

r_{33} and r_{13} are the electro-optic coefficients. E_{PR} is the light-induced space-charge electric field. The birefringence changes are represented as $\Delta n_{PR} = (\Delta n_e - \Delta n_o)$. The corresponding phase-retardation changes between orthogonal polarizations of a propagating light are expressed as

$$\Delta\phi_{PR} = (2\pi/\lambda)\Delta n_{PR} L, \tag{2}$$

where $L = 4$ cm is the crystal length, and $\lambda = 633$ nm is the wavelength of probe light. The relation is further represented by $\Delta n_{PR} = \Delta\phi_{PR} \times 2.5 \times 10^{-6}$. Δn_{PR} can be obtained by measuring the phase variations $\Delta\phi_{PR}$. Moreover, the time-varying phase variations $\Delta\phi_{PR}$ (t) can be used to calculate the photorefractive sensitivity as defined by [10]

$$S_{PR} = [d\Delta n_{PR}(t)/dt]/I|_{t=0}, \tag{3}$$

where I is the irradiated power intensity, and the time derivate of the birefringence change $d\Delta n_{PR}(t)/dt$ is obtained by considering the measured data in the initial period.

3. RESULTS AND DISCUSSION

The output beam of ZIPM through the lens L2 can be focused to a beam diameter of 80 μm along the test crystal at a wavelength of 633 nm. The power intensity is 50 W/mm^2 for the throughput power of 25 μW measuring behind the Mg:LN. Figure 2 shows the measured phase variations for the sensing and reference channels at a power intensity of 50 W/mm^2. The dynamical ranges of the phase variations are 0.003 and 0.96 rad for the reference and sensing channels, respectively. The results show that the reference-phase variations from the ZIPM are near-stable. However, the sensing phase variations through the Mg:LN crystal are obvious. This means that the power intensities from the ZIPM are enough to characterize the light-induced birefringence. Figure 3(a) illustrates the light-induced birefringence changes versus irradiated time for different power intensities. These measured birefringence curves show an oscillating phenomena with different amplitudes and damping periods, which are dependent on the power intensities. The time derivate of the birefringence change $d\Delta n_{PR}(t)/dt$ is obtained by considering the data within the initial 30 s as shown in Figure 3(b). The slops of the best-fit birefringence changes versus time can be used to calculate S_{PR}. According to Eq. (3), the calculated S_{PR} and $d\Delta n_{PR}(t)/dt$ are shown in Figure 4. The calculated S_{PR} is at a same level within a power intensity range from 20 to 50 W/mm^2. However, S_{PR} is a little high at a relative low intensity of 10 W/mm^2. This error data was caused due to the difficulty of obtaining correct slops, as shown in the measured data of 10 W/mm^2 of the Figure 3(b). We believe that this power intensity is a detection limit for S_{PR}. The methodology provides the resolution of S_{PR} measurements as low as 10^{-10} mm^2/J.

The light-induced birefringence can be modulated by irradiating with another shorter-wavelength pump light of 532 nm. In this measurement, the probe red-light intensity is 50 W/cm^2, and

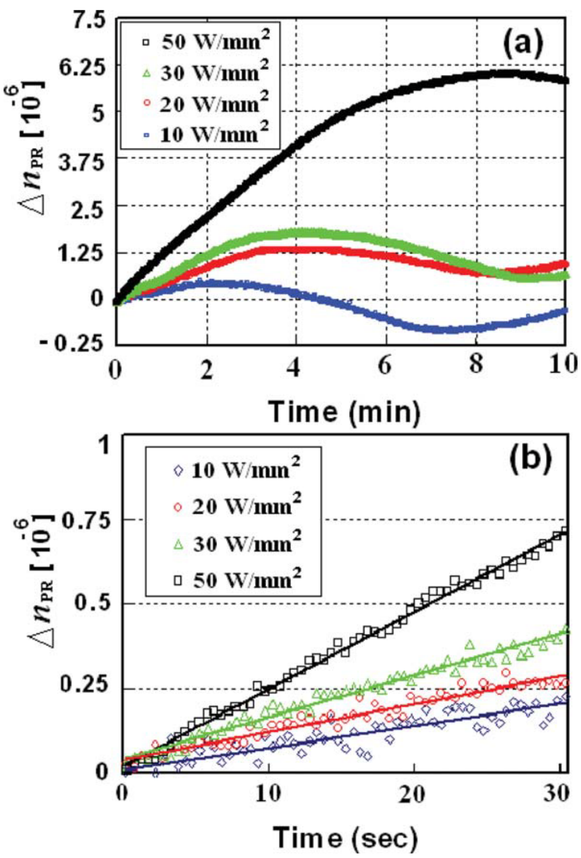

Figure 3 Birefringence changes as a function of time for different throughput power intensities: (a) time duration of 10 min and (b) initial 30 s. [Color figure can be viewed in the online issue, which is available at wileyonlinelibrary.com]

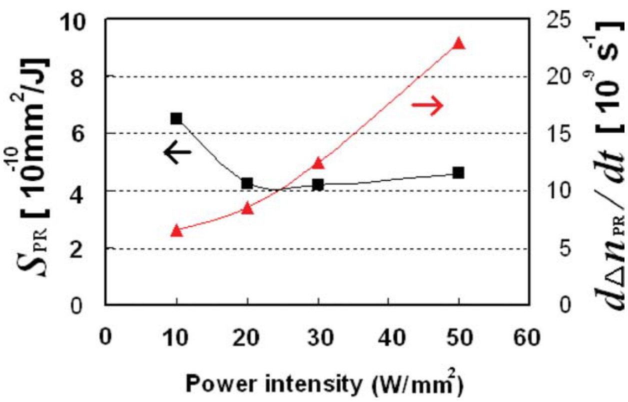

Figure 4 S_{PR} and $d\Delta n_{PR}/dt$ as a function of power intensities. [Color figure can be viewed in the online issue, which is available at wileyonlinelibrary.com]

the pump green-light intensity is 5 W/mm^2 (beam diameter = 1 mm). Similar to the measurements by periodically irradiating with the pump light [6], the pump light is periodically blocked at a period of 30 s with a mechanical shutter in this study. Figure 5(a) gives the dynamical birefringence changes under the periodical changes of the pump light. The pump light is switched off in the initial period of 30 s. However, the continuously increased birefringence is caused by the probe red light itself.

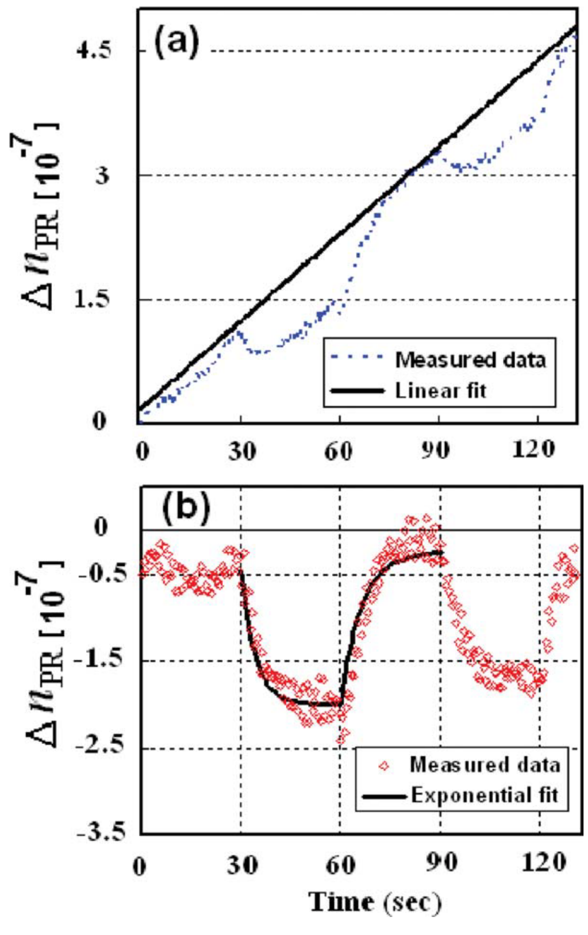

Figure 5 Birefringence changes versus time under the periodical pump green light: (a) originally measured data and (b) subtraction between measured data and linear fit. [Color figure can be viewed in the online issue, which is available at wileyonlinelibrary.com]

The linear fit in Figure 5(a) is simulated for the birefringence changes induced by the probe light. The pump light is switched on at time $t = 30$ and 90 s. The illuminations of pump light will erase already exited space-charge distributions in the crystals [11]. Therefore, the birefringence change is decreased gradually. After switching off the pump light at time $t = 60$ and 120 s, the birefringence change is increased again. By subtracting the birefringence changes induced from the probe light, Figure 5(b) shows the results of subtraction between the measured data and the linear fit [given in Fig. 5(a)]. The processed data represent the similarly exponential tendency as presented in [6]. The detection of Δn_{PR} at the level of 10^{-7} is lower than the conventional Senarmont compensation method [6, 7]. Therefore, we can use lower pump intensities of 532 nm to characterize the only light-induced birefringence changes while avoiding the thermally-induced birefringence changes as discussed in [6].

4. CONCLUSIONS

In summary, to our knowledge, we have introduced a novel light-induced birefringence measurement scheme, which uses an integrated ZIPM for phase modulation in homodyne metrology. We showed that the proposed configuration provides extremely low-detection limits to a photorefractive sensitivity of 10^{-10} mm^2/J and birefringence change of 10^{-7} at a probe light of 633-nm wavelength. The proposed methodology makes possible ultrasensitive measurements under a relatively simple experimental arrangement and can be applied for studying the PRE in $LiNbO_3$ and $LiTaO_3$ crystals.

ACKNOWLEDGMENTS

This work was supported in part by the National Science Council of Taiwan (NSCT), under Grant NSC 98-2221-E-218-006.

REFERENCES

1. P. Gunter and J.-P. Huignard, Photorefractive materials and their applications 2, Springer, Berlin, 2006.
2. R.K. Banyal and B.R. Prasad, Holographic recording in Fe:Ce:Ti:-$LiNbO_3$ crystal, Opt Commun 274 (2007), 300–306.
3. F. Juvalta, R. Mosimann, M. Jazbinsek, and P. Gunter, Fast dynamic waveguides and waveguide arrays in photorefractive $Sn_2P_2S_6$ induced by visible light, Opt Express 19 (2009), 379–384.
4. M. Chauvet, V. Coda, H. Maillotte, E. Fazio, and G. Salamo, Large self-deflection of soliton beams in $LiNbO_3$, Opt Lett 30 (2005), 1977–1979.
5. O. Matoba, T. Inujima, T. Shimura, and K. Kuroda, Segmented photorefractive waveguides in $LiNbO_3$:Fe, J Opt Soc Am B 15 (1998), 2006–2012.
6. L. Razzari, P. Minzioni, I. Cristiani, V. Degiorgio, and E.P. Kokanyan, Photorefractivity of Hafnium-doped congruent lithium-niobate crystals, Appl Phys Lett 86 (2005), 131914.
7. M. Falk, Th. Woike, and K. Buse, Reduction of optical damage in lithium-niobate crystals by thermo-electric oxidation, Appl Phys Lett 90 (2007), 251912.
8. R.C. Twu, H.Y. Hong, and H.H. Lee, Dual-channel optical phase measurement system for improved precisions, Opt Lett 33 (2008), 2530–2532.
9. R.C. Twu, H.Y. Hong, and H.H. Lee, An optical homodyne technique to measure photorefractive-induced phase drifts in lithium niobate phase modulators, Opt Express 16 (2008), 4366–4374.
10. E.P. Kokanyan, L. Razzari, I. Cristiani, V. Degiorgio, and J.B. Gruber, Reduced photorefraction in hafnium-doped single-domain and periodically poled lithium niobate crystal, Appl Phys Lett 84 (2004), 1880–1882.
11. Y. Liu, L. Liu, D. Liu, L. Xu, and C. Zhou, Intensity dependence of two-center nonvolatile holographic recording in $LiNbO_3$:Cu:Ce crystals, Opt Commun 190 (2001), 339–343.